Greener Journal of Physical Sciences

ISSN: 2276-7851 Impact Factor 2012 (UJRI): 0.7799 ICV 2012: 5.88

Comparison of 2D and 3D Resistivity Imaging Methods in the Study of Shallow Subsurface Structures

By

Hussein Abdelwahab

Research Article

Comparison of 2D and 3D Resistivity Imaging Methods in the Study of Shallow Subsurface Structures

Hussein Abdelwahab

Department of Physics, College of Education, University of Mustansiryah.

Email: hususm@uomustansiriyah.edu.iq, Tel: 00964-7711660885

Abstract

2D and 3D resistivity imaging methods are simple, fast, inexpensive, and relatively accurate techniques used in geophysics exploration. In this study, 2D and 3D resistivity imaging methods are used to produce images of the subsurface structure of the University of Technology in Baghdad, Iraq. Three 2D images are utilized to create a 3D slice image and a 3D block image for three conventional arrays. Each 2D image has a length of 60m and a depth of approximately 12m, and the spacing between lines is 1.5m. Results show that the study area consists of two types of material: sandy gravel and clay. The borehole data obtained near the study area are used to confirm the results. The 2D and 3D images, as well as the three conventional arrays, are compared. Wenner array is found to be the most suitable array for 2D and 3D imaging of the study area.

Keywords: Electrical resistivity imaging.

INTRODUCTION

Humans explore subsurface structures, such as environmental, agricultural, and archeological structures, for numerous reasons. The most common method to explore subsurface areas is bore-holing, which is a significantly accurate method. However, bore-holing is not always suitable for all targets because it produces limited data and damages the study area; its use is also expensive and relatively time consuming [Ekinci and Kaya, 2007]. Geophysical techniques are instead employed to avoid these disadvantages of bore-holing. Many geophysical methods are available, with each of these methods having its respective advantages and disadvantages depending on the target study area and the type of the area [Aizebeokhai, 2010]. Examples of geophysical techniques are the 2D and 3D electrical resistivity imaging methods. These methods are accurate in determining complex subsurface structures, effective in detecting ground water, cavities and pipes, and relatively inexpensive. The user-friendly and portable equipment used in 2D and 3D electrical resistivity methods can cover long distances [Hussein, 2010]. However, the results obtained with the use of these methods are less accurate than those obtained via bore-holing. Selecting an unreliable array also further reduces the accuracy of results. The use of 3D images is the most accurate geophysical method to represent the real world, which is 3D.

This study aims to reduce the disadvantages of using 2D resistivity imaging. This aim is achieved through a comparison of the results of common conventional arrays with those of borehole data to select a suitable array. Furthermore, a 3D image of the study area is created to obtain accurate information on the subsurface structure of the area. Most studies have compared arrays with the use of 2D imaging, whereas only a few have used 3D imaging.

Borehole data (Table 1) indicate that the surface layer of the study area consists of sandy, silt clay with a thickness of 1m to 3m. The silt clay layer comes after the surface layer until a depth of 10m, where the amount of sand nearly equals that of clay. The third layer consists of sand only.

Table 1: Borehole data obtained near the study area

	BH1			
Depth (m)	**Clay (%)**	**Silt (%)**	**Sand (%)**	**Gravel (%)**
1.5	47	28	15	10
3.0	41	29	12	8
4.5	-	-	-	-
6.0	51	46	3	0
7.5	52	42	6	0
9.0	52	46	2	0
10.5	59	36	5	0
12.0	-	-	-	-
15.0	-	-	-	-
	BH2			
1.5	41	31	18	10
3.0	52	46	2	0
4.5	48	47	5	0
6.0	57	40	3	0
7.5	55	41	4	0
9.0	56	40	4	0
10.5	63	35	2	0
12.0	-	-	-	-
15.0	-	-	-	-

Figure 1 shows the study area in the main garden of the University of Technology in Baghdad, Iraq.

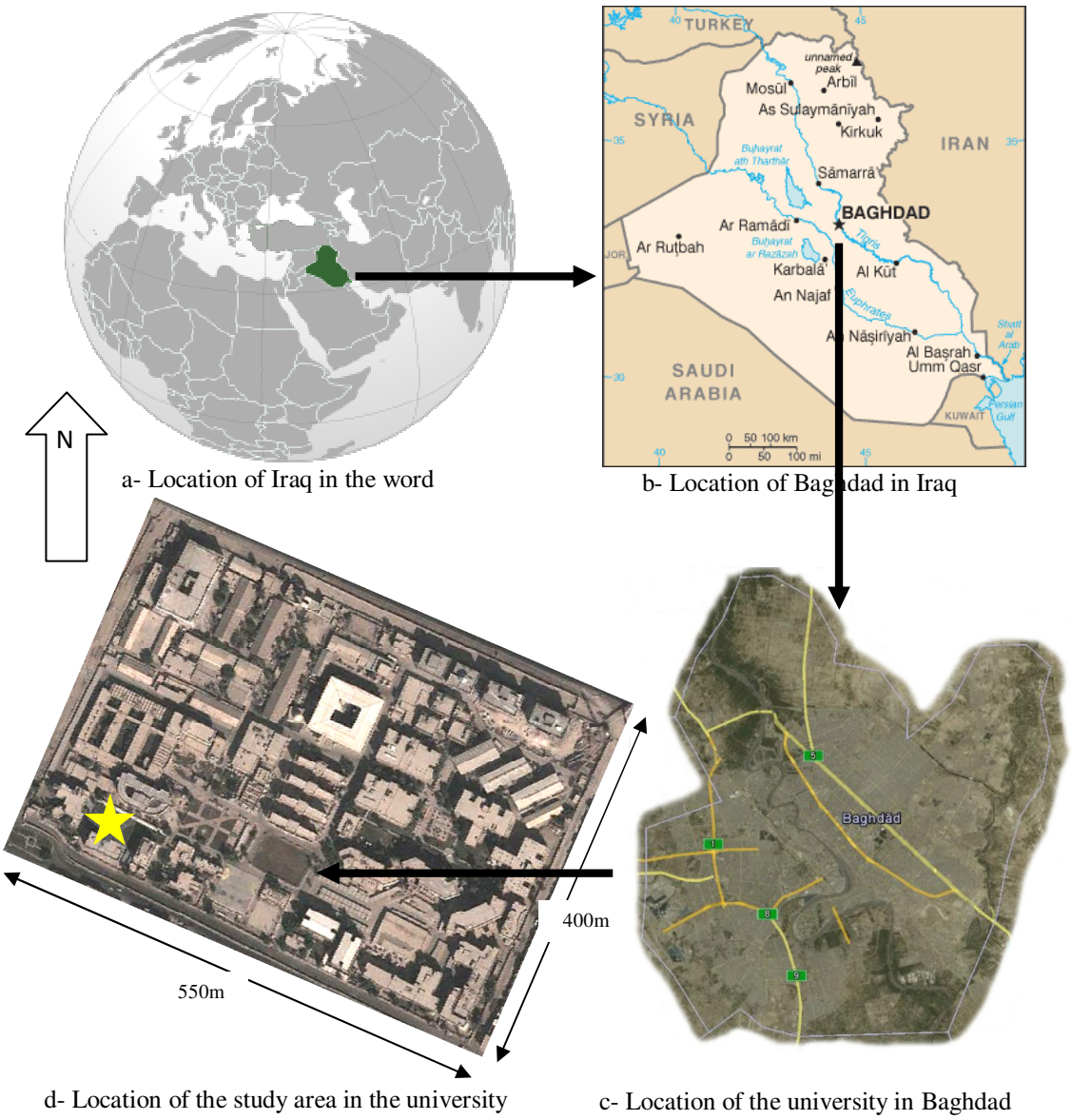

Figure 1: Location of the study area.

Resistivity imaging technique

Most surveys on modern electrical resistivity aim to obtain the true resistivity values of subsurface structures because true resistivity is geologically significant. Resistivity imaging technique depends on Ohm's law, which states that the electric current (I) in a material is proportional to the potential difference across it. The linear relationship between these two variables is expressed by the following equation:

$$V = I R, \quad (1)$$

Where (I) is the current, (V) is the potential difference, and (R) is the resistance. The above equation is the linear relationship between (V) and (I). For a given material, resistance is proportional to length (L) and inversely proportional to the cross-sectional area (A) of the conductor. These relationships are expressed in the following equation:

$$R = \rho L / A. \quad (2)$$

The proportionality constant (ρ) is the resistivity of the conductor. Resistivity, a physical property of materials, is the ability to resist a flow of charges; it is the measurement of how strongly a material resists the flow of electric current [Denchik and Chapellier, 2005].

Ohm's Law states that, "For many materials (including most metals), the ratio of the current density to the electric field is a constant σ that is independent of the electric field producing the current" [Serway and Jewett, 2007].

$$J = \sigma E \text{ (Ohm's Law)} \quad (3)$$

The constant of proportionality (σ) is the conductivity of the material, (J) is the current density, and (E) is the electric field. The inverse of conductivity is resistivity (ρ):

$$E = \rho J. \quad (4)$$

For a homogeneous area with one electrode, the potential separates radially away from the current source, where the area (A) is a half sphere ($2\pi r^2$) with radius (r). Equation 2 is rewritten as

$$\rho = R K, \quad (5)$$

Where $K = 2 \pi r$ for a half sphere. Equation 5 consists of two parts. The first part is resistance (R) and the second part is geometric factor (K), which describes the geometry of the electrode configuration.

Figure 2 shows that for a homogeneous area with two couples of electrodes, the geometric factor in Equation 5 is a variable that depends on the type of electrode configuration.

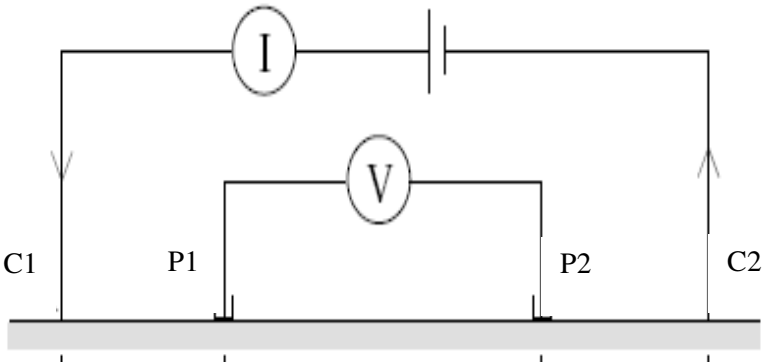

Figure 2: General four-electrode configuration for resistivity measurement

The geological structures of the ground are inhomogeneous, and the obtained values of resistivity represent apparent resistivity instead of true resistivity [Lowrie, 2007; Reynolds, 1997]. Therefore, the resistivity (ρ) in Equation 5 changes to apparent resistivity (ρ_a) in an inhomogeneous area:

$$\rho_a = R K. \quad (6)$$

Equation 6 is used to calculate apparent resistivity, which depends on the type of subsurface structure and the arrangement of current electrodes and voltage poles. True resistivity can be calculated from apparent resistivity with the use of RES2DINV, a commercial software that uses numerical methods to estimate true resistivity and plot a 2D or 3D image [Loke, 2011].

Terrameter SAS 4000, an automatic electric imaging device, is used in this study. This system injects current into the surface with the use of two electrodes that read the potential difference between two other electrodes. Depending on the type of array used in the survey, the system then calculates the resistance R and apparent resistivity. Figure 3 shows that electrode selector ES10-64, a multichannel relay matrix switch connected to Terrameter SAS 4000 is used for electrical resistivity imaging. In addition, 2 spread cables, 41 stainless steel electrodes and 42 jumpers are used along with Terrameter SAS 4000.

Figure 3: Tools and equipment used in the study.

The 3D slice resistivity images are created from three separate lines. Each line is a 2D resistivity image with a length of 60 m and with 42 electrodes. The distance between the lines is 1.5m. The 3D block images are then created by using Slice Dicer software.

RESULTS AND DISCUSSION

The results (Figures 4, 5, and 6) of this study are used to create 2D images with RES2DINV software. The 2D images were then combined into 3D slice images (Figure 7) with RES3DINV software. The 3D slice images were converted to 3D block images (Figure 8) with Slicer Dicer software. The 3D images consist of three dimensions: x-axis, y-axis, and z-axis, which refer to length (60m), width (3m), and depth (approximately 15m), respectively. The color in the image indicates the resistivity values of the subsurface structure of the study area.

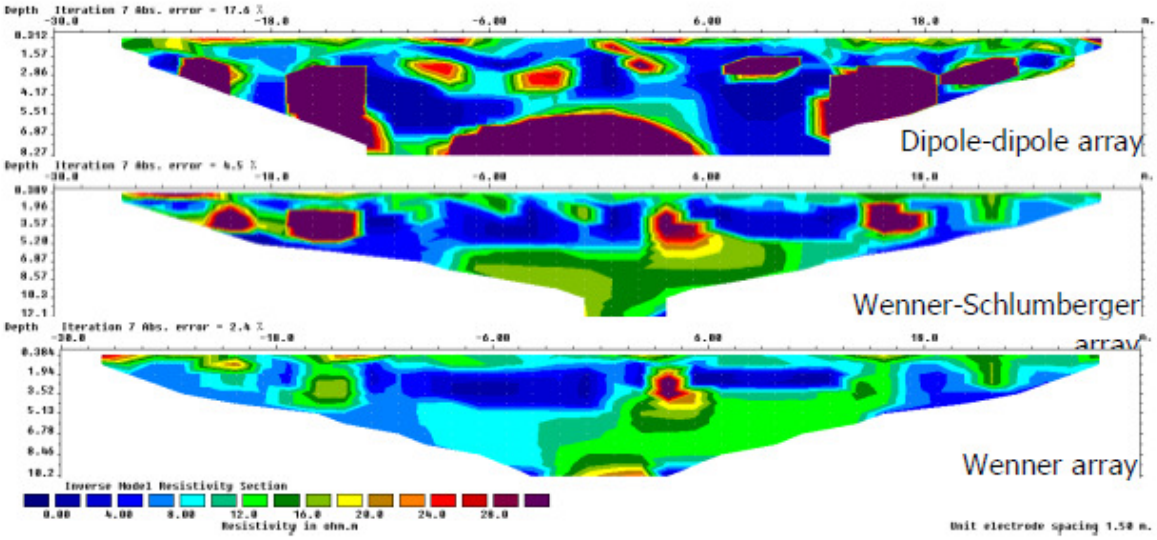

Figure 4: 2D images for Line 1 with the use of dipole-dipole, Wenner-Schlumberger, and Wenner arrays.

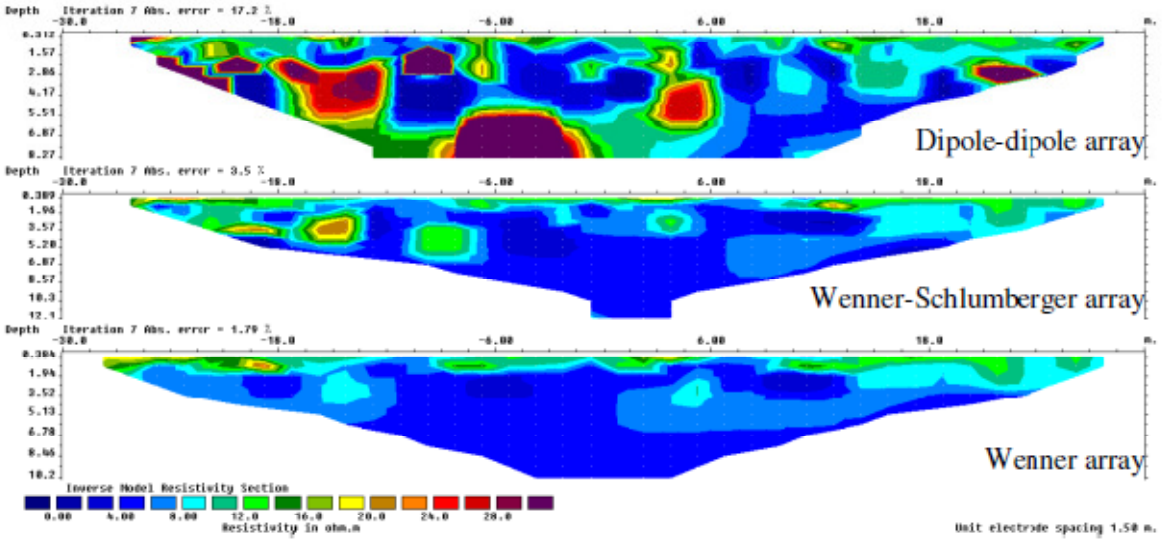

Figure 5: 2D images for Line 2 with the use of dipole-dipole, Wenner-Schlumberger, and Wenner arrays.

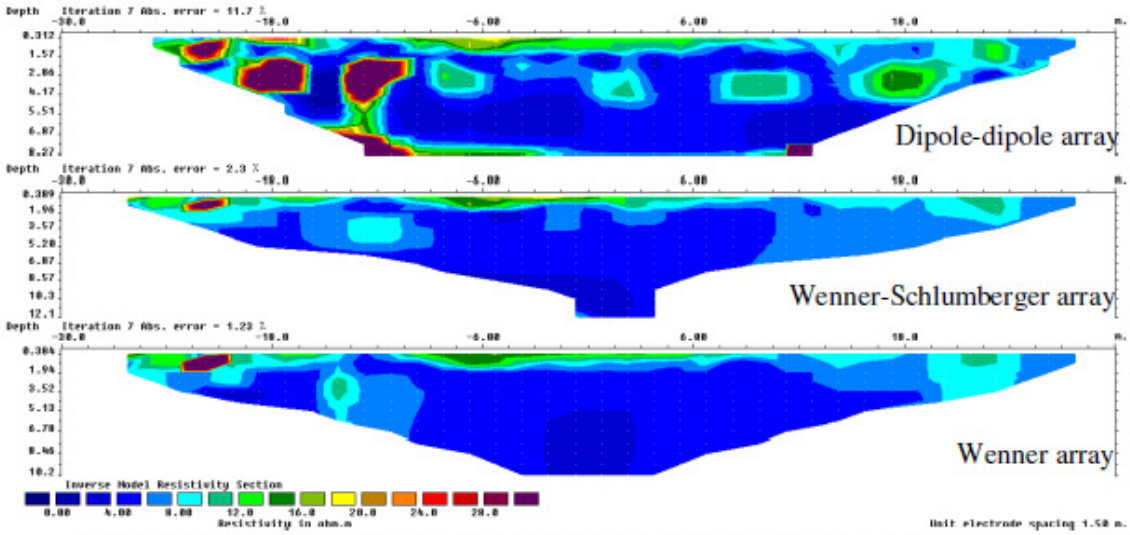

Figure 6: 2D images for Line 3 with the use of dipole-dipole, Wenner-Schlumberger, and Wenner arrays.

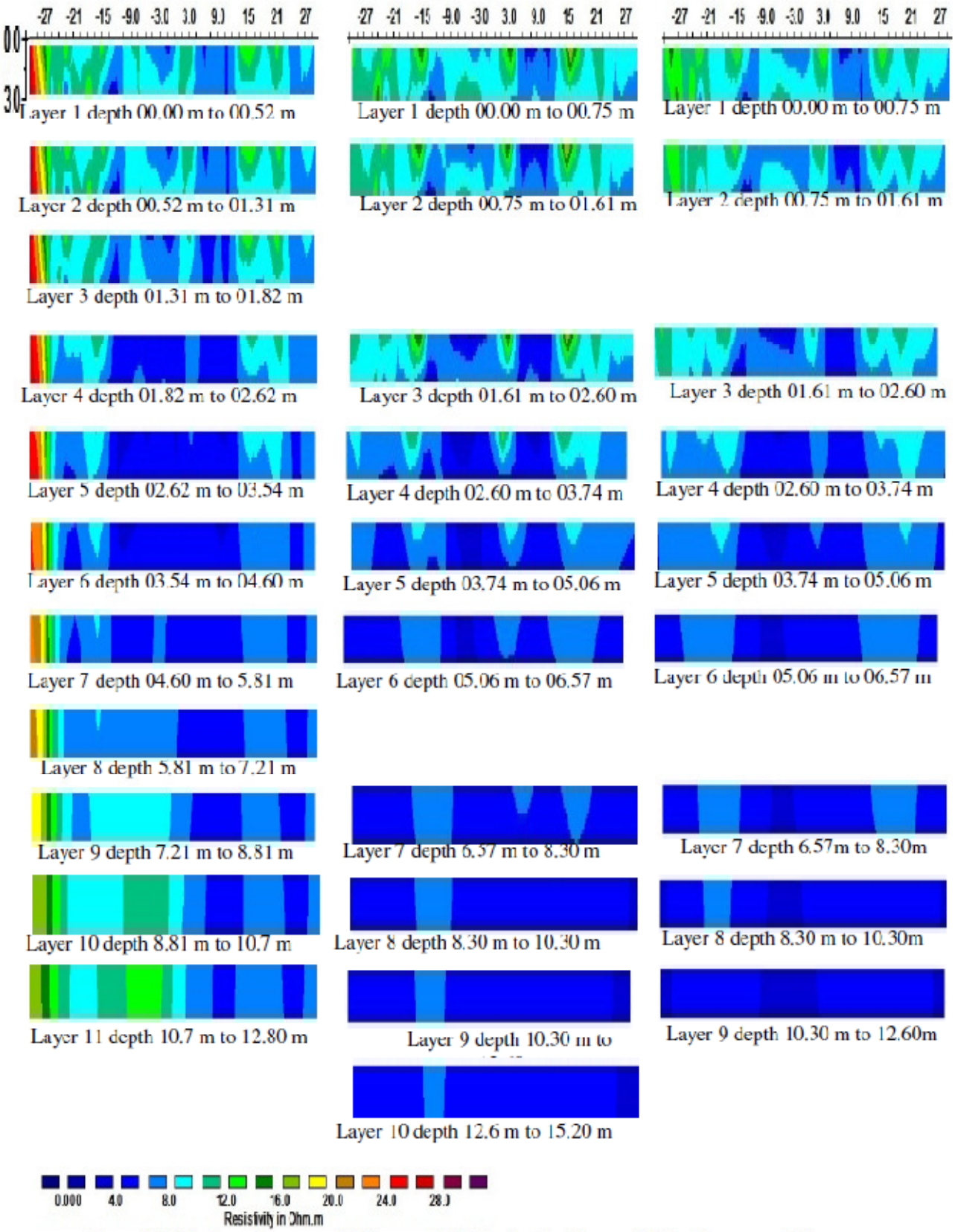

Figure 7: Slice layer images with the use of dipole-dipole, Wenner-Schlumberger, and Wenner arrays.

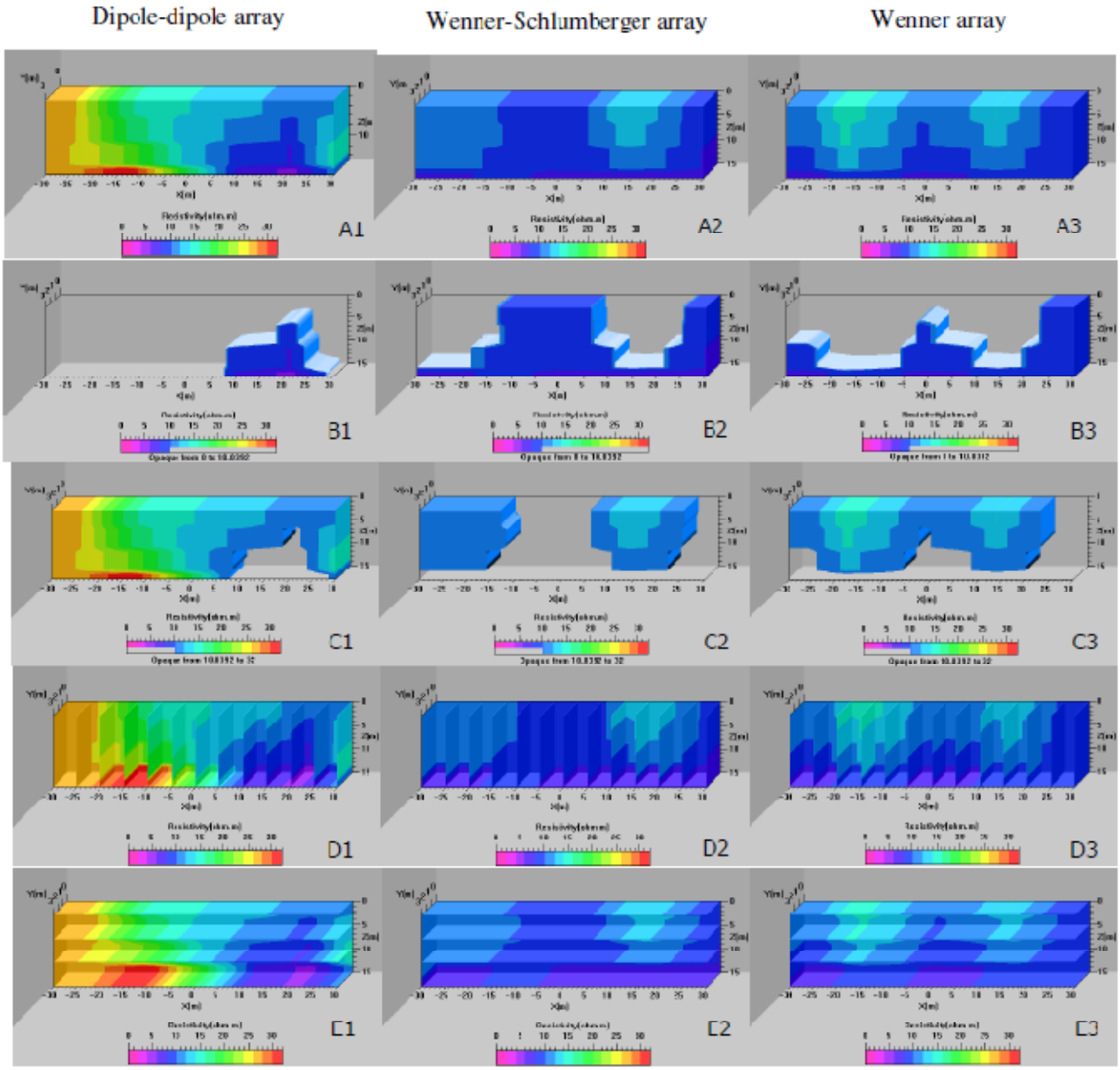

Figure 8: 3D images with the use of dipole-dipole (column 1), Wenner-Schlumberger (column 2), and Wenner arrays (column 3).

Figures 7 and 8 shows that a 3D image can summarize numerous 2D images into a single image. Using a 3D image to image subsurface structure is easy and results in significantly clear and realistic interpretations because subsurfaces have three dimensions in reality.

Table 2: Resistivity values of common materials found in the study area

Material	Resistivity (Ω.m)	Resistivity (Ω.m) of the subsurface from the 3D resistivity image	Resistivity (Ω.m) of the subsurface from the 2D resistivity image
Alluvium and sand	10–800	10–30	
Clay (sand free)	1–10	0–10	

Table 3: Maximum resistivity of the three lines and arrays

	Maximum resistivity values in the 2D images (Ω.m)		
2D image	Dipole-dipole array	Wenner-Schlumberger array	Wenner array
Line 1	1347	110	38
Line 2	282	23	23
Line 3	1774	47	95
	Maximum resistivity values in the 3D images (Ω.m)		
3D image	29	18	14

The 2D image results show that the maximum resistivity values of Line 1 are 1347, 110, and 38 Ω.m with the use of dipole-dipole, Wenner-Schlumberger, and Wenner arrays, respectively (as shown in Table 3 and Figures 4, 5, and 6). The maximum resistivity values of Line 2 are 282, 23, and 23 Ω.m with the use of dipole-dipole, Wenner-Schlumberger, and Wenner arrays, respectively. The maximum resistivity values of Line 3 are 1774, 47, and 95 Ω.m with the use of dipole-dipole, Wenner-Schlumberger, and Wenner arrays respectively. The maximum value for all lines and arrays is 1774 Ω.m. The 3D image results show that the maximum resistivity values are 29, 18, and 14 Ω.m with the use of dipole-dipole, Wenner-Schlumberger, and Wenner arrays respectively. The maximum value for all arrays is 29 Ω.m. The 2D and 3D image results differ because the 3D images are created from combined 2D images. The 2D images are of poorer quality than the 3D images created from complete 3D images (Loke, 2011).

The borehole data (Table 1) show that the structure of the study area consists of alluvium and sand at the top layer and clay at the second layer, where the mean of the resistivity values (as shown in Table 2) should range from 10 Ω.m to 800 Ω.m for the top layers and from 0 Ω.m to 10 Ω.m for the second layers. Moreover, the maximum resistivity value cannot exceed 800 Ω.m. Therefore, the 2D results of the dipole-dipole array are beyond the range of the expected resistivity values. In addition, the 3D results of the dipole-dipole array show that the study area has a clay upper layer followed by a sandy layer (Figure 8C1), a composition that is opposite that of the real structure.

The results of the 2D (Figure 4, 5, and 6) and 3D images (Figure 7 and 8) show that the resistivity values of the study area could be classified into two ranges: the low resistivity range, which lies between 0 Ω.m and 10 Ω.m, and the second range, which is from 10 Ω.m and above.

The above results are interpreted according to the data obtained from a nearby borehole (Table 1) and the material resistivity values (Table 2). A low resistivity value ranging from 0 Ω.m to10 Ω.m is interpreted as clay, whereas a high resistivity value above 10 Ω.m is interpreted as top soil (sandy, silt, and gravelly). The high resistivity value of the top soil layer decreases as the clay value increases until the layer becomes only clay (free soil).

The Wenner-Schlumberger array used in 2D and 3D imaging can penetrate deeper than the other arrays. Otherwise, the accuracy and identification ability of the Wenner array are most similar with the borehole data results, in which the Wenner array indicates that most areas of the top layer have high resistivity values. This finding suggests a sandy layer, as shown in Figures 8, 8B3, and 8C2.

CONCLUSION:

The dipole-dipole array cannot be used for 2D and 3D imaging in the study area. The Wenner-Schlumberger array is a good choice for researchers if depth of penetration is required in the target area. By contrast, the Wenner array is a good choice if a fast work speed or many lines are required in the target area. In general, the Wenner array is the most suitable array in the study area examined for 2D and 3D electrical resistivity mapping.

ACKNOWLEDGMENT

The author is grateful to the University of Technology for allowing him to conduct the study in the university. The researcher also thanks the Unit of Remote Sensing and GIS of the Department of Building and Construction Engineering for allowing him to use their equipment.

REFERENCES

Aizebeokhai, A. P. (2010). 2D and 3D Geoelectrical resistivity imaging: Theory and field design. Scientific Research and Essays, 5(23), 3592-3605.

Denchik, N., & Chapellier, D. (2005). 3D electrical resistivity monitoring during rainfalls. Paper presented at the 3rd Swiss Geoscience Meeting.

Ekinci, Y. L., & Kaya, M. A. (2007). 3D resistivity imaging of buried tombs at the Parion necropolis. Journal of the balkan geophysics society, 10(2), 1-8.

Hussein Abdelwahab Moussa (2010). The use of GIS and resistivity imaging techniques to determine landslide probability based on internal and external causal factors. Ph.D. thesis, 2010, University Sains Malaysia, Penang, Malaysia, University SAINS Malaysia, Penang.

Loke, M. H. (2011). Rapid 3D Resistivity & IP inversion using the least-squares method: Geoelectrical Imaging 2D & 3D Geotomo software.

Lowrie, W. (2007). Fundamentals of Geophysics (2 ed.): Cambridge University Press.

Reynolds, J. M. (1997). An Introduction to Applied and Environmental Geophysics: John Wiley & Sons, Ltd.

Serway, R. A., & Jewett, J. W. (2007). Physics for Scientists and Engineers (6 ed.): Thomson Brooks / Cole.